

Air Flow-Assisted Ionization Imaging Mass Spectrometry Method for Easy Whole-Body Molecular Imaging under Ambient Conditions

Zhigang Luo,^{†,||} Jiuming He,^{†,||} Yi Chen,[‡] Jingjing He,[†] Tao Gong,[‡] Fei Tang,[‡] Xiaohao Wang,[‡] Ruiping Zhang,[†] Lan Huang,[§] Lianfeng Zhang,[§] Haining Lv,[†] Shuanggang Ma,[†] Zhaodi Fu,[†] Xiaoguang Chen,[†] Shishan Yu,[†] and Zeper Abliz*,[†]

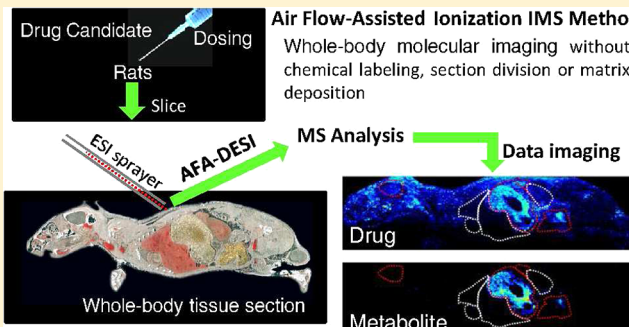
[†]State Key Laboratory of Bioactive Substance and Function of Natural Medicines, Institute of Materia Medica, Chinese Academy of Medical Sciences and Peking Union Medical College, Beijing 100050, People's Republic of China

[‡]State Key Laboratory of Precision Measurement Technology and Instruments, Department of Precision Instruments and Mechanology, Tsinghua University, Beijing 100084, People's Republic of China

[§]Institute of Laboratory Animal Science, Chinese Academy of Medical Sciences and Peking Union Medical College, Beijing 100021, People's Republic of China

Supporting Information

ABSTRACT: Whole-body molecular imaging is able to directly map spatial distribution of molecules and monitor its biotransformation in intact biological tissue sections. Imaging mass spectrometry (IMS), a label-free molecular imaging method, can be used to image multiple molecules in a single measurement with high specificity. Herein, a novel easy-to-implement, whole-body IMS method was developed with air flow-assisted ionization in a desorption electrospray ionization mode. The developed IMS method can effectively image molecules in a large whole-body section in open air without sample pretreatment, such as chemical labeling, section division, or matrix deposition. Moreover, the signal levels were improved, and the spatial assignment errors were eliminated; thus, high-quality whole-body images were obtained. With this novel IMS method, *in situ* mapping analysis of molecules was performed in adult rat sections with picomolar sensitivity under ambient conditions, and the dynamic information of molecule distribution and its biotransformation was provided to uncover molecular events at the whole-animal level. A global view of the differential distribution of an anticancer agent and its metabolites was simultaneously acquired in whole-body rat and model mouse bearing neuroglioma along the administration time. The obtained drug distribution provided rich information for identifying the targeted organs and predicting possible tumor spectrum, pharmacological activity, and potential toxicity of drug candidates.



Molecular imaging techniques have received considerable attention and have advanced to become invaluable tools for molecular biology research,^{1–3} drug design,⁴ disease diagnosis,^{5–7} and therapy assessment.⁸ Whole-body molecular imaging, an extension of biological tissue imaging, can present a broad picture of the biological state both healthy and diseased by directly mapping molecular spatial distribution and monitoring complex biochemical processes involved in an intact biosystem.⁹ Determining the localization of drug molecules in a whole-body animal plays a fundamental role in drug discovery because drug localization affects the pharmacological and toxicological responses.⁴ Whole-body autoradiography (WBA) is a well-developed molecular imaging technology for analyzing the drug distribution in whole-body tissue sections. However, radioactive labeling and loss of chemical specificity restrict WBA to differentiating parent drugs and metabolites. Imaging mass spectrometry (IMS),^{9–12} a label-free imaging technique integrating spatial distribution with

molecular specificity for mapping multiple targeted or non-targeted molecules, opens numerous avenues in biomedical research. IMS techniques mainly include secondary ion mass spectrometry (SIMS) imaging,^{13,14} matrix-assisted laser desorption/ionization (MALDI) imaging,^{15,16} and ambient molecular imaging initiated by desorption electrospray ionization (DESI),^{17,18} matrix-assisted laser desorption electrospray ionization (MALDESI),^{19,20} laser ablation electrospray ionization (LAESI),^{21–23} and low-temperature plasma (LTP)²⁴ probe.

MALDI-IMS is an important tool for biomarker discovery and assessing drug disposition directly from tissue sections.^{16,25} As for whole-body MALDI imaging, a large section is divided into four smaller ones due to the limited vacuum sample

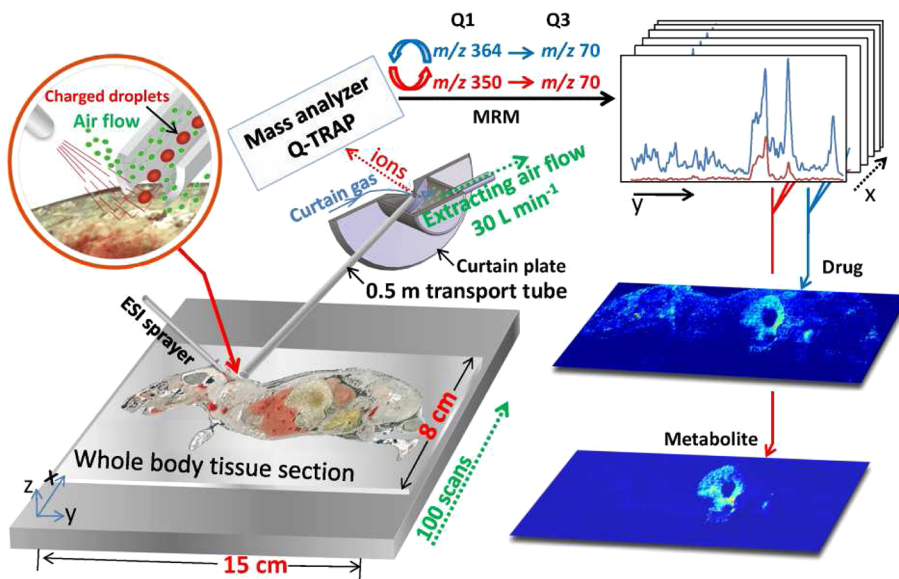
Received: January 1, 2013

Accepted: February 5, 2013

Published: February 5, 2013



Scheme 1. AFADESI-Based Strategy to Develop an Easy-to-Implement, Label-Free IMS Method for the Molecular Imaging of Multiple Target Molecules in a Large Whole-Body Tissue Section under Ambient Conditions



space.^{12,25–27} In addition, the matrix is critical for the generation of sufficient analyte ions but causes sample movement, which leads to spatial assignment errors. As a recently developed ambient ionization technique,^{24,28,29} DESI does not involve a matrix or extensive sample preparation and has been successfully applied for drugs and metabolites,¹⁸ lipids,³⁰ fingerprint chemical imaging,³¹ and so forth. Moreover, some remote sampling methods coupled to DESI^{32–34} and MALDESI³⁵ were developed and applied on homeland security detection, environmental monitoring, and so forth. However, the imaging of large whole-body sections challenges ambient ionization sources equipped close to the MS orifice. The signal level will decrease with increasing length of a simple extended MS orifice or capillary³⁶ because atmospheric pressure and gas flow significantly affect the transfer and focus of ions.

An effective method is needed to improve the signal level, eliminate spatial assignment errors, and ensure the quality of whole-body imaging.^{9,12,18} This paper presents a novel IMS technique that attempts to map the molecular spatial distribution easily at the whole-body level by using the air flow-assisted ionization in DESI mode (AFADESI) under ambient conditions. As one of the ambient ionization techniques, AFA ionization (AFAI) was suitable for the MS analysis of large objects in open air because the high flow-rate extracting air flow was introduced to improve ion collection and remote transport efficiency and to promote charged droplets desolvation.³⁷ It also has demonstrated that gas flows is effective to collect ions and transfer them over long distances for mass spectrometric analysis.³⁸ As the ionization process of DESI, an electrospray plume was directly impacted on the sample surface, where it desorbed and ionized molecules from the tissue section. But then, the AFADESI technique did improve the sensitivity of ambient MS analysis of large objects. Herein, we have designed and tested the AFADESI-IMS method that is highly effective for imaging multiple molecules in a large whole-body section. Scheme 1 shows the strategy to do that. This AFADESI-IMS method demonstrated that it was easy-to-implement and label-free for whole-body imaging without sample pretreatment (e.g., chemical labeling, section

division, or matrix deposition) and eliminated obstacles in the path toward better understanding of molecular events at the whole-animal level.

The AFADESI-IMS method succeeded in global visual analysis of the disposition of an anticancer drug candidate in rat and tumor model mouse tissue sections, which were affixed at 500 mm from the MS analyzer. It was demonstrated that this method can map the targeted drug molecule with picomolar sensitivity in an ambient environment, and use of a high extracting air flow rate eliminated ion contamination and diffusion between consecutive sampling pixels.

■ EXPERIMENTAL SECTION

Materials and Instruments. Formic acid was purchased from Sigma-Aldrich (St. Louis, MO). High-performance liquid chromatography (HPLC)-grade methanol and acetonitrile were purchased from Merck (Muskegon, MI). Pure water (Wahaha, Hangzhou, China) was obtained from a local market. Ammonia solution was purchased from Beijing Chemical Factory (Beijing, China). The antitumor candidate drug S-(+)-deoxytlyphorinidine (CAT) was obtained from Prof. Shishan Yu (Institute of Materia Medica, Chinese Academy of Medical Sciences). CAT was prepared as a 3 mg mL⁻¹ aqueous solution in 0.9% NaCl. Rhodamine B was purchased from Sinopharm Chemical Reagent Company Limited, and basic blue 7 was extracted from a blue pen (Zebra), which was obtained from a local market. Rhodamine B and basic blue 7 were dissolved in a mixture of methanol and water (4:1, v/v), and the solutions were used in place of inks in an inkjet printer. Male Wistar rats (weighing 148–170 g) were purchased from the Institute of Laboratory Animal Science, Chinese Academy of Medical Sciences.

All IMS experiments were completed using a QTRAP 5500 mass spectrometer (AB SCIEX Foster City, CA) equipped with a custom-made AFAI ion source. Sagittal whole-body cryosections were prepared using a Leica CM3600 cryomacrotome (Leica Microsystems Ltd., Germany).

For details on animal handling and whole-body tissue section preparation, see the Supporting Information.

Experimental Setup and AFADESI-IMS Configuration. The AFADESI-IMS system and the experimental setup are shown in Figure S1 (Supporting Information). The AFAI ion source was constructed with a stainless steel transport tube (i.d. 3 mm, o.d. 4 mm, length 500 mm), a custom-made PMMA refluence tube (i.d. 16 mm, length 60 mm) that was used to pump back the air flow and was fixed to the mass spectrometer, a flow meter (0–65 L min⁻¹, Tianjian Flow Meter Co., Tianjian, China), and a vacuum pump. The stainless steel transport tube was placed at a 60° angle to the central axis of the MS orifice. The exit of the transport tube was sealed to the refluence tube. The vertical distance between the outlet of the transport tube and the MS orifice was set at ~3 mm. The straight line distance was typically set at 10 mm. A 15° wedge-shaped opening was designed to approach the surface of the tissue section. The interval between the tube mouth and section surface was set at 0.3 mm. The sampling end of the transport tube was brought into the proximity of the desorption region of the tissue section to collect the secondary charged droplets containing analytes. The air exit of the refluence tube was connected to the flow meter, and air was extracted by the vacuum pump with a narrow bore pipe (i.d. 8 mm, o.d. 12 mm).³⁷ The vacuum pump was used to generate a high air flow rate in the AFAI system.

In the sampling desorption region, an ESI sprayer (o.d. 150 μm, i.d. 100 μm) was used to generate the initial charged droplets for the desorption of substance in the tissue section. The sprayer was mounted on a manual three-dimensional (3D) translational stage with a 55° spray angle to allow positioning relative to the transport tube and tissue surface with submillimeter precision. The distance between the sprayer and the surface of the tissue section was set at 0.6 mm. The distance between the sprayer and the sampling end of the transport tube was set at 3 mm.

A tissue section was fixed on a glass slide, which was mounted on an electric 3D translational stage (MTS225, Beijing Optical Instrument Factory, Beijing, China) to allow automatic control of its position with submillimeter precision. The electric 3D translational stage was controlled by custom-developed software, by which a trigger signal was sent to the MS to synchronize MS analysis with the programmed movement of the stage.

IMS Analysis. All IMS experiments were performed with a custom-made AFAI ion source in DESI mode. The spray gas was N₂, the flow rate was 2 L min⁻¹, and the spray voltage was 5000 V. The spray solution was prepared by mixing methanol and water (4:1, v/v) with 0.1% formic acid. It was delivered to the sprayer by an Agilent LC pump at a flow rate of 10 μL min⁻¹. The extracting air flow was set at 35 L min⁻¹.

For the MS parameters, the source temperature was set at heat off, and gas 1 and gas 2 were all set at 0. The curtain gas and the declustering potential were set at 20 arb (1.7 L min⁻¹) and 55 V, respectively. The transport tube voltage was the same as the voltage applied on the curtain plate. The collision gas was set at high. The collision energy was set at 50 eV. Nitrogen gas was used as the curtain gas and the collision-active dissociation (CAD) gas. MS/MS analysis utilized multiple reaction monitoring (MRM) for CAT (*m/z* 364.2 → 70.0) and its metabolite M1 (*m/z* 350.2 → 70.0) enabling a very specific and sensitive response for the detection of selected analytes of interest, and the dwell time was set at 200 ms. These transition settings were established according to the MS spectra and

product ion spectra of CAT and M1 (Supporting Information, Figure S2).

Molecular imaging experiments were conducted in a unidirectional scanning mode by continuously moving the surface of the sagittal section in the *y* direction at 400 μm s⁻¹. At the beginning of each lane, a signal triggered the waiting MS to acquire raw MS/MS data. One scan was summed for each pixel in the image, with an MS dwell time of 200 ms. The step size in the *x* direction was 500 μm, and the target area was 143 mm × 48 mm resulting in the collection of 883 by 96 data points; thus, each pixel in the image is 500 μm × 162 μm. After the end of each lane scan, the surface was lowered in the *z* direction by 2 mm. The tissue was returned to the start position of the subsequent lane at 10 mm s⁻¹ to avoid contamination of the unanalyzed tissue regions. Data acquisition and processing were performed with Analyst software, version 1.5.1. Raw MS/MS data of individual lane scans were stored in separate data files.

Investigation of the AFADESI-IMS Assembly. Experiments were conducted to investigate the effect of two key parameters on the signal intensity, the length of the transport tube and the extracting air flow rate. Four transport tubes of different lengths (300, 500, 1000, and 3000 mm) were selected. (For experimental details, see the Supporting Information.)

Investigation of Spatial Resolution and “Carry-Over”.

Two important aspects of IMS, carry-over and spatial resolution, were evaluated using AFAI with the 500 mm transport tube. An alternating pattern of red and blue bars and a pattern of different red bars at different intervals were used as the test case. Mass data were acquired in the same scan mode as in the IMS experiments. (For experimental details, see the Supporting Information.)

Data Processing and Imaging. Data processing and imaging were performed using custom-developed software based on Matlab 7.0 (Mathworks, Natick, MA). Acquired raw data were stored in wiff format by Analyst 1.5.1. Each chromatograph of MRM was saved as a text file with two columns after smoothing. All of the text files were loaded into Matlab 7.0. The first column of the text file was the MS scan time (min), which was transformed as the *y* axis for imaging output (Y position, mm) according to the IMS scan rate. The second column containing the ion intensity information of the consecutive unidirectional lane scans was combined into one matrix for data imaging (data matrix). The *x* axis for imaging output was calculated according to the formula *X* = number of IMS scans × step size, *X* position (mm). The data matrix was visualized with the *x* and *y* axes by the functions “imagesc” and “plot tools” in Matlab 7.0. The figure was modified in “plot tools” and output as the molecular image.

RESULTS AND DISCUSSION

Evaluation of Sensitivity, Spatial Resolution, and Spatial Assign Errors of AFADESI-IMS. Whole-body IMS experiments require enough space to perform high sensitivity and accuracy of MS analysis or location on image of spatial assignment to guarantee the imaging quality. It was reported that signal levels could be affected by one or more of the following reasons: ion suppression, low desorption/ionization efficiency, and inefficient droplet/ion collection and transport into the mass spectrometer.³⁶ Most of the parameters for desorption/ionization of the AFADESI-MS system were referred to in our previously reported work³⁷ and other related DESI techniques.³⁶ Herein, we focused on the ion collection

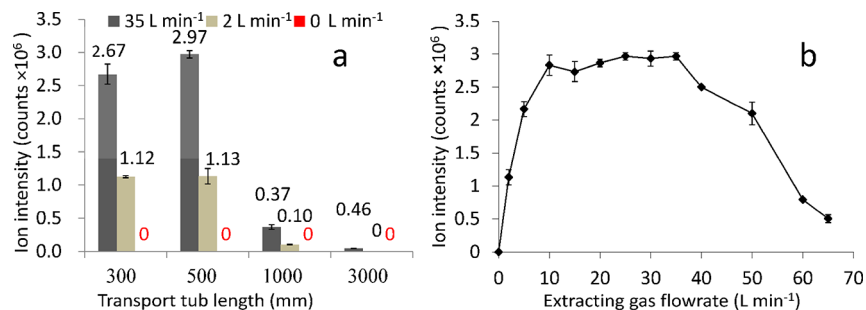


Figure 1. Optimization of the transport tube length and the extracting gas flow rate in AFADESI-IMS for whole-body imaging. (a) Ion intensity for Rhodamine B solution (m/z 443) in mass spectra acquired with transport tubes of different lengths (300, 500, 1000, and 3000 mm). (b) Ion intensity of Rhodamine B (m/z 443) vs the extracting air flow rate, with the 500 mm transport tube.

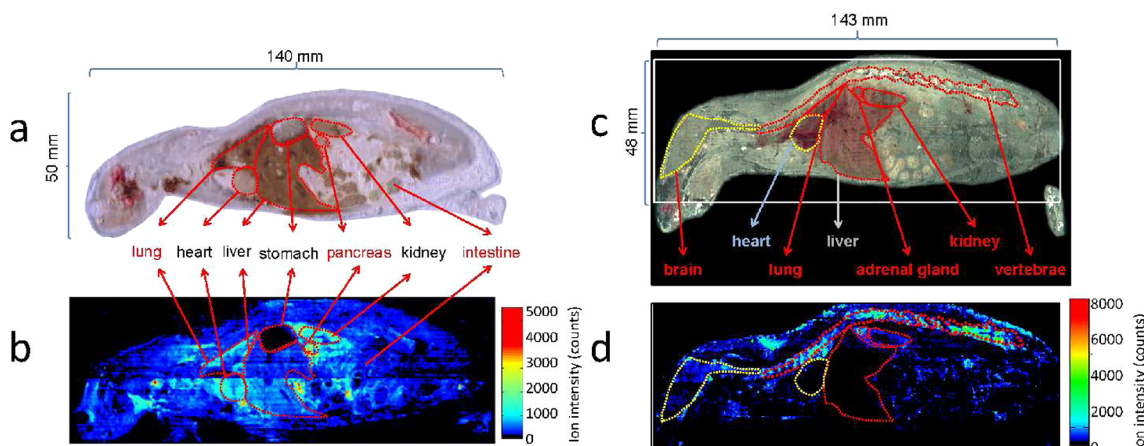


Figure 2. CAT distribution in rat acquired by whole-body AFADESI-IMS. (a, c) Two optical images of 40 μ m thick sagittal sections from the different layers of a rat (dosed intravenously with 10 mg kg⁻¹ CAT) euthanized 20 min after dosing. Organ regions are outlined. (b, d) AFADESI-IMS images of CAT (MRM, m/z 364.2 \rightarrow 70.0) in a and c. Spatial resolution is 300 μ m \times 500 μ m.

and the transport efficiency, especially considering the long transport distance. In this AFADESI-IMS system, high extracting air flow was introduced to enable high sensitivity with a long transport tube that can provide enough sampling space. The results of the investigation on tube length and air flow rate (Figure 1) showed that, when the extracting air flow rate increased from 0 to 10 L min⁻¹ (the flow meter was installed on the outlet line of the system), the ion intensity in the MS spectra increased significantly, and when the air flow rate ranged from 10 to 40 L min⁻¹, the ion intensity remained high and relatively stable subsequently. These results further indicated that high sensitivity of remote IMS analysis for large whole-body imaging could be obtained even with a long transport tube and curtain gas interface. In AFADESI-IMS, the extracting air flow rate and the transport tube length were optimized at 30 L min⁻¹ and 500 mm, respectively, which provided high sensitivity and sufficient space for easily mapping large tissue sections. In this condition, a high signal level above background was observed for the target drug molecule and even the trace of metabolites.

Furthermore, to guarantee the quality of whole-body imaging, “carry-over” and spatial resolution were evaluated with the optimized transport tube length and the extracting air flow rate, with details shown in the Supporting Information. The results (Supporting Information, Figure S5) demonstrated that the main reason for the carry-over is the size of the ESI plume, which would bring about partial crossover on the boundary, not the length of transport tube, because the

transport time for desorbed analytes transported to the MS orifice is so fast that ion accumulation and diffusion can be avoided (transport time calculated as 0.007 s with extracting air flow at 30 L min⁻¹). Therefore, the high extracting air flow rate eliminated ion contamination and diffusion, two reasons for “carry-over” between consecutive sampling pixels.

It was reported that, after systematic optimizations of emitter capillary size, solvent composition, solvent flow rate, mass spectrometry scan rate, and step size, the spatial resolution of the IMS experiment with a DESI source can be significantly improved to resolve precise structure of small biological tissues.³⁹ Considering that the requirement of drug distribution analysis is just to resolve certain substructures of organs in a whole-body IMS experiment, along with the compromise of sampling time, sample stability, and sensitivity, an ESI sprayer with a spatial resolution of 300 μ m was selected, and an acceptable step was set at 500 μ m. At this resolution, it took 9 h to analyze a target area for IMS (5 cm \times 14 cm). (Evaluation of spatial resolution was shown in the Supporting Information.)

In addition, the transport tube placed at a 60° angle to the central axis of the MS orifice was designed to prevent ablated pieces of tissue from blocking the orifice of the mass spectrometer, thus improving the stability of IMS experiments.

Therefore, owing to the high extracting air flow, the AFADESI-IMS method provides enough sample space, high sensitivity, and accuracy for whole-body IMS experiments at the same time. In addition, using this method, a large whole-body section can be mapped in an easy-to-implement way in one

experiment without small-part division and matrix deposition, which are necessary for MALDI-IMS.^{12,25–27}

Whole-Body Imaging of Drug Disposition. Figure 2 shows the results for the whole-body imaging of the anticancer drug candidate CAT⁴⁰ acquired by AFADESI-IMS in MRM scan mode. The images clearly show the distributions of CAT (estimated as ~0.1 ng per sampling point: choosing the CAT content in kidney that the lowest content can be detected by AFADESI-IMS method and dividing the content obtained with quantitative LC-MS/MS by the approximate size of rat kidney, then multiplying the volume of a sampling point) in whole-body rat tissue sections compared to the complex background noise. Different organs were exposed on tissue sections because of the different layers. The two tissue sections from a rat (Figure 2a,c) were imaged in order to display comprehensive information about drug distribution in various organs. Direct visual comparison between the IMS images and the optical images revealed a global view of the differential distribution of drug and metabolite simultaneously in various organ regions. High CAT concentrations were observed in the pancreas, adrenal gland, vertebrae, lung, brain, kidney, and intestine; low concentrations were found in the heart and liver. Moreover, subregional variations of intensity were clearly observed within the same organ, such as the skull, medulla oblongata, and cerebrum (Figure 2a,c). The CAT content in organs was further determined by quantitative LC-MS/MS (Figure 3 and

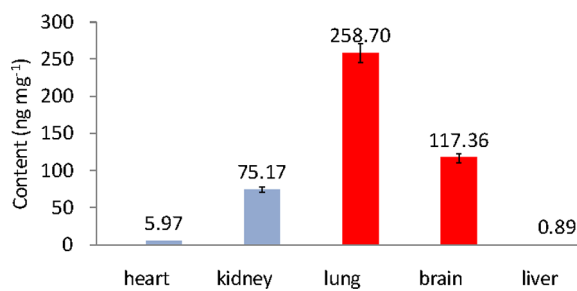


Figure 3. CAT content in individual organs of rats euthanized 20 min after dosing, measured by quantitative LC-MS/MS.

quantitative test of individual organ tissue by LC-MS/MS in the Supporting Information). Consistent results between LC-MS/MS and IMS confirmed the feasibility and reliability of the AFADESI-IMS method for drug disposition analysis.

The dynamic status of CAT during its biotransform was determined with AFADESI-IMS by comparing the whole-body images at 20 min (Figure 2) and 2 h (Figure 4b,c) after dosing. After 2 h, CAT was steadily conserved in the brain, adrenal gland, and kidney. CAT was readily metabolized into M1 in the stomach and intestine, where it accumulated and was excreted (Figure 4b,c).

CAT disposition was evaluated in a mouse bearing a neuroglioma (Figure 4d) with the AFADESI-IMS method. At 2 h after tail vein injection of 5 mg kg⁻¹ CAT, the disposition of CAT (results in Figure 4e,f) was consistent with that obtained in a normal rat. High CAT concentrations were observed in the stomach, intestine, and subcutaneous fat. M1 accumulation was seen in the stomach and intestine. Importantly, CAT showed enrichment in the tumor region, suggesting that CAT accumulated in the tumor regions via transport through the rich vascular network.

Pharmacological Implications. Pharmacodynamics and pharmacokinetics data demonstrated that CAT possesses potent cytotoxicity activity to glioma, pancreatic cancer, and lung cancer cells in vitro and can penetrate the blood–brain barrier.⁴⁰ The high quality images obtained by the AFADESI-IMS method were the same as the previous results, further indicating that CAT may potentially be developed as an antitumor drug for the treatment of glioma and pancreatic and lung cancers without serious hepatic lesion. Targeted CAT accumulation was observed in the tumor regions of the model mouse. The concentrated distributions of CAT and M1 in the stomach and intestine provided a possible explanation for the diarrhea and weight loss observed in CAT-treated animals. The results also gave clues to the metabolic specificity and mechanism of action of CAT.

CONCLUSION

The easy-to-implement IMS method developed with AFAI in DESI mode can map multiple targeted molecules in large

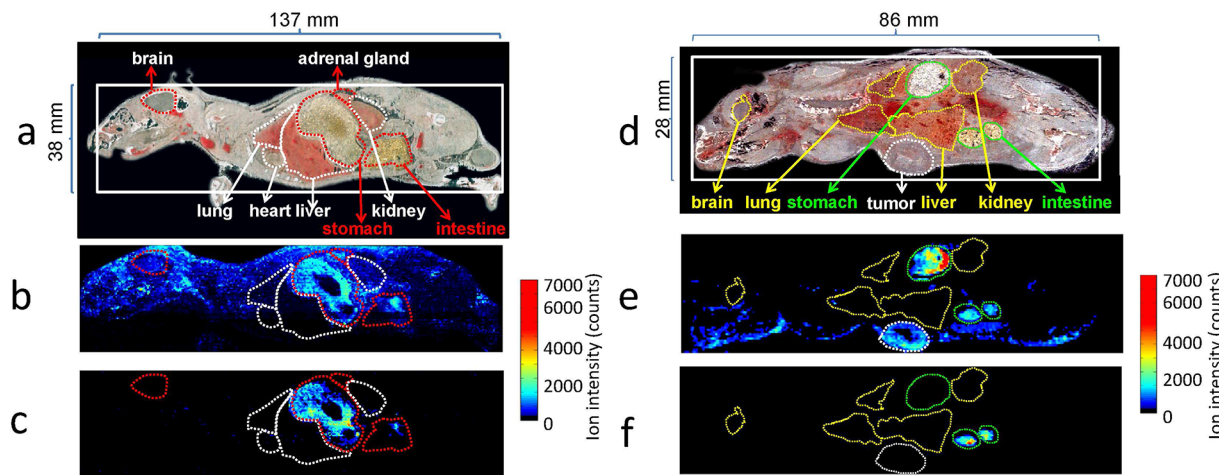


Figure 4. CAT and M1 distributions in rat and mouse bearing neuroglioma acquired by whole-body AFADESI-IMS. Optical images of 40 μ m thick sagittal sections of rat (dosed intravenously with 10 mg kg⁻¹ CAT) and model mouse (dosed intravenously with 5 mg kg⁻¹ CAT) euthanized 2 h (a, d) after dosing. Organ regions are outlined. (b, e) AFADESI-IMS images of CAT (MRM, m/z 364.2 \rightarrow 70.0) in a and d. (c, f) AFADESI-IMS images of M1 (MRM, m/z 350.2 \rightarrow 70.0) in a and d. Spatial resolution is 300 μ m \times 500 μ m.

whole-body tissue sections without matrix deposition, section division, and high-vacuum conditions. Meanwhile, this method overcame the contradiction between the sample size and enough sensitivity faced by the whole-body IMS experiment. Such a highly sensitive whole-body IMS method easily operated under ambient conditions undoubtedly is valuable, since it not only provides enough sampling space but also guarantees high sensitivity during remote ion transportation. By achieving both aspects simultaneously, it will improve the understanding of molecular events at the whole-animal level.

The global visual information about drug disposition obtained by AFADESI-IMS allows the direct discovery of the organs targeted by drug candidates and can predict the tender tumor-spectrum to anticancer agents. In addition, this IMS method might evolve into a powerful tool for predicting pharmacological activity and potential toxicity.

■ ASSOCIATED CONTENT

Supporting Information

Additional information as noted in the text. This material is available free of charge via the Internet at <http://pubs.acs.org>.

■ AUTHOR INFORMATION

Corresponding Author

*E-mail: zeper@imm.ac.cn.

Author Contributions

[†]These authors contributed equally to this work.

Notes

The authors declare no competing financial interest.

■ ACKNOWLEDGMENTS

The authors thank Professor Robert J. Cotter (Johns Hopkins University) and Professor Huanwen Chen (East China Institute of Technology) for enlightening discussions. The authors thank the National Instrumentation Program (2011YQ170067) and the National Scientific and Technological Major Project for New Drugs (2012ZX09301002-001-006) for financial support.

■ REFERENCES

- (1) Steinhauser, M. L.; Bailey, A. P.; Senyo, S. E.; Guillermier, C.; Perlstein, T. S.; Gould, A. P.; Lee, R. T.; Lechene, C. P. *Nature* **2012**, *481*, 516–519.
- (2) Hong, G. S.; Wu, J. Z.; Robinson, J. T.; Wang, H. L.; Zhang, B.; Dai, H. J. *Nat. Commun.* **2012**, *3*, 700–708.
- (3) Qian, Y.; Karpus, J.; Kabil, O.; Zhang, S. Y.; Zhu, H. L.; Banerjee, R.; Zhao, J.; He, C. *Nat. Commun.* **2011**, *2*, 495–501.
- (4) Willmann, J. K.; Bruggen, N. V.; Dinkelborg, L. M.; Gambhir, S. S. *Nat. Rev. Drug Discovery* **2008**, *7*, 591–601.
- (5) Kircher, M. F.; Zerda, A.; Jokerst, J. V.; Zavaleta, C. L.; Kempen, P. J.; Mittra, E.; Pitter, K.; Huang, R. M.; Campos, C.; Habte, F.; Sinclair, R.; Brennan, C. W.; Mellinghoff, I. K.; Holland, E. C.; Gambhir, S. S. *Nat. Med.* **2012**, *18*, 829–834.
- (6) Kircher, M. F.; Willmann, J. K. *Radiology* **2012**, *263*, 633–643.
- (7) Gamhir, S. S. *Nat. Rev. Cancer* **2002**, *2*, 683–693.
- (8) O'Connor, J. P. B.; Jackson, A.; Parker, G. J. M.; Roberts, C.; Jayson, G. C. *Nat. Rev. Clin. Oncol.* **2012**, *9*, 167–177.
- (9) Reyzer, M. L.; Chaurand, P.; Angel, P. M.; Caprioli, R. M. *Mass Spectrometry Imaging: Principles and Protocols*; Springer: New York, 2010; Vol. 656.
- (10) Watrous, J. D.; Dorrestein, P. C. *Nat. Rev. Microbiol.* **2011**, *9*, 683–694.
- (11) Cornett, D. S.; Reyzer, M. L.; Chaurand, P.; Caprioli, R. M. *Nat. Methods* **2007**, *4*, 828–833.
- (12) Vickerman, J. C. *Analyst* **2011**, *136*, 2199–2217.
- (13) Kaganman, I. *Nat. Methods* **2006**, *3*, 962–963.
- (14) Kim, Y. P.; Oh, E.; Oh, Y. H.; Moon, D. W.; Lee, T. G.; Kim, H. S. *Angew. Chem., Int. Ed.* **2007**, *46*, 6816–6819.
- (15) Schwamborn, K.; Caprioli, R. M. *Nat. Rev. Cancer* **2010**, *10*, 639–646.
- (16) Sinha, T. K.; Shahidi, S. K.; Yankeelov, T. E.; Mapara, K.; Ehtesham, M.; Cornett, D. S.; Dawant, B. M.; Caprioli, R. M.; Gore, J. C. *Nat. Methods* **2008**, *5*, 57–59.
- (17) Wiseman, J. M.; Ifa, D. R.; Venter, A.; Cooks, R. G. *Nat. Protoc.* **2008**, *3*, 517–524.
- (18) Wiseman, J. M.; Ifab, D. R.; Zhu, Y. X.; Kissinger, C. B.; Manicke, N. E.; Kissinger, P. T.; Cooks, R. G. *Proc. Natl. Acad. Sci. U.S.A.* **2008**, *105*, 18120–18125.
- (19) Sampson, J. S.; Hawkridge, A. M.; Muddiman, D. C. *J. Am. Soc. Mass Spectrom.* **2006**, *17*, 1712–1716.
- (20) Sampson, J. S.; Hawkridge, A. M.; Muddiman, D. C. *J. Am. Soc. Mass Spectrom.* **2008**, *19*, 1527–1534.
- (21) Nemes, P.; Barton, A. A.; Li, Y.; Vertes, A. *Anal. Chem.* **2008**, *80*.
- (22) Nemes, P.; Vertes, A. *J. Visualized Exp.* **2010**, *43*, 1–4.
- (23) Nemes, P.; Barton, A. A.; Vertes, A. *Anal. Chem.* **2009**, *81*, 6668–6675.
- (24) Liu, Y. Y.; Ma, X. X.; Lin, Z. Q.; He, M. J.; Han, G. J.; Yang, C. D.; Xing, Z.; Zhang, S. C.; Zhang, X. R. *Angew. Chem., Int. Ed.* **2010**, *49*, 4435–4437.
- (25) Khatib-Shahidi, S.; Andersson, M.; Herman, J. L.; Gillespie, T. A.; Caprioli, R. M. *Anal. Chem.* **2006**, *78*, 6448–6456.
- (26) Stoeckli, M.; Staab, D.; Schweitzer, A. *Int. J. Mass Spectrom.* **2007**, *260*, 195–202.
- (27) Trim, P. J.; Henson, C. M.; Avery, J. L.; McEwen, A.; Snel, M. F.; Claude, E.; Marshall, P. S.; West, A.; Princivalle, A. P.; Clench, M. R. *Anal. Chem.* **2008**, *80*, 8628.
- (28) Takats, Z.; Wiseman, J. M.; Gologan, B.; Cooks, R. G. *Science* **2004**, *306*, 471–473.
- (29) Cooks, R. G.; Ouyang, Z.; Takats, Z.; Wiseman, J. M. *Science* **2006**, *311*, 1566–1570.
- (30) Eberlin, L. S.; Dill, A. L.; Golby, A. J.; Ligon, K. L.; Wiseman, J. M.; Cooks, R. G.; Agar, N. Y. *Angew. Chem., Int. Ed.* **2010**, *49*, 5953–5956.
- (31) Ifa, D. R.; Manicke, N. E.; Dill, A. L.; Cooks, R. G. *Science* **2008**, *321*, 805–805.
- (32) Cotte-Rodriguez, I.; Cooks, R. G. *Chem. Commun.* **2006**, *28*, 2968–2970.
- (33) Cotte-Rodriguez, I.; Mulligan, C. C.; Cooks, R. G. *Anal. Chem.* **2007**, *79*, 7069–7077.
- (34) Dixon, R. B.; Bereman, M. S.; Muddiman, D. C.; Hawkridge, A. M. *J. Am. Soc. Mass Spectrom.* **2007**, *18*, 1844–1847.
- (35) Dixon, R. B.; Sampson, J. S.; Hawkridge, A. M.; Muddiman, D. C. *Anal. Chem.* **2008**, *80*, 5266–5271.
- (36) Kertesz, V.; Van Berkel, G. J.; Marissa, V.; Koeplinger, K. A.; Schneider, B. B.; Covey, T. R. *Anal. Chem.* **2008**, *80*, 5168–5177.
- (37) He, J. M.; Tang, F.; Luo, Z. G.; Chen, Y.; Xu, J.; Zhang, R. P.; Wang, X. H.; Abiliz, Z. *Rapid Commun. Mass Spectrom.* **2011**, *25*, 843–850.
- (38) Garimella, S.; Xu, W.; Huang, G. M.; Harper, J. D.; Cooks, R. G.; Ouyang, Z. *J. Mass Spectrom.* **2012**, *47*, 201–207.
- (39) Campbell, D. I.; Ferreira, C. R.; Eberlin, L. S.; R. Cooks, R. G. *Anal. Bioanal. Chem.* **2012**, *404*, 389–398.
- (40) Lv, H. N.; Ren, J. H.; Ma, S. G.; Xu, S.; Qu, J.; Liu, Z. J.; Zhou, Q.; Chen, X. G.; Yu, S. S. *PLoS One* **2012**, *7*, 1–16.